

Field Study and Simulation of Geochemical Mechanisms of Soil Alkalinization in the Sahelian Zone of Niger

S. MARLET

Unité de Recherche Gestion de l'Eau
CIRAD-CA
Montpellier, France

V. VALLES

Station de Science du Sol
INRA
Montfavet, France

L. BARBIERO

ORSTOM
Niamey, Niger

In some soils of the Niger valley, alkalinization and sodization are related to the concentration of alteration products of calco-alkaline gneiss to biotite, which releases significant amounts of cations and alkalinity. The result is an oversaturation of the soil solution with respect to calcite, which precipitates with a positive calcite residual alkalinity. Ca^{2+} molality decreases, while alkalinity and pH increase; Ca^{2+} desorption is accompanied by adsorption of Na^+ on the exchange complex. K^+ , Mg^{2+} , and Na^+ concentrations in the soil solution are successively controlled by the formation of illites and smectite-type silicates, while kaolinite dissolves. These processes were successfully simulated according to the analytical data. They agreed with the significant increase of the alkaline reserve in the soils according to chemical, physical, and mineralogical alterations. These geochemical mechanisms were found to be involved in the formation of alkali soils at three sites of the region.

Keywords alkalinity, alkali soil, calcite, geochemistry, Niger River, silicate, sodium

Increasing use of irrigation enables the expansion of cultivable land and intensification of agricultural production, which spawn sizable production increases in the alluvial and fossil valleys of the Sahel. However, in some cases, water supply may not be the major limiting factor of production because of the occurrence of alkalinization and sodization, which result in low fertility and poor soil structure.

Felspar dissolving and kaolinite-type clay precipitation are involved in the production

Received 16 December 1994; accepted 18 October 1995.

Address correspondence to S. Marlet, CIRAD-CA, Unité de Recherche Gestion de l'Eau, BP 5035, 34032 Montpellier, France.

243

Arid Soil Research and Rehabilitation, 10:243-256, 1996
Copyright © 1996 Taylor & Francis
0890-3069/96 \$12.00 + .00

Fonds Documentaire ORSTOM



010015430

Fonds Documentaire ORSTOM

Cote: B * 15430 Ex: 1

of alkalinity and the genesis of alkali soils (Tardy, 1985). Alkalinity is equal to the sum of the concentrations of the weak bases multiplied by the number of protons that each base can neutralize, minus the proton concentration of the solution (Bourrié, 1976). For most soils, alkalinity is due to carbonate (HCO_3^-) species. When a solution is concentrated by evaporation up to the point that calcite (CaCO_3) precipitates, alkalinity and Ca^{2+} molality cannot increase together. In case Ca^{2+} equivalents exceed alkalinity equivalents in the original soil solution, alkalinity decreases and Ca^{2+} molality increases. In a reverse situation, alkalinity increases and Ca^{2+} molality decreases. This concept of residual sodium carbonates (RSC) was described by Eaton (1950) and is now referred to as residual alkalinity (RA). RA has been generally used with respect to the precipitation of calcite (calcite residual alkalinity, or C-RA) and allows prediction of how water quality changes while it concentrates. Valles et al. (1991) showed that C-RA is an invariant criterion for irrigation water quality assessment. The concept has been generalized to the successive precipitation of several minerals (van Beek & van Breemen, 1973; Droubi, 1976).

In an alkaline environment, Si can be involved in silicate precipitation, which has accounted for the dissolved Si and Mg behavior in models (Gac et al., 1977; Guedarri, 1984; Vallès et al., 1989). Nevertheless, these minerals were at variance with field observations. Furthermore, cation exchange simulation and other species such as potassium or sodium generally were not considered.

This article considers how soils become alkaline and sodic under natural conditions. Considering that Ca, Mg, K, and Na are controlled by the precipitation of calcite and silicate minerals and ion exchanges, the processes involved in alkalization were simulated.

Materials and Methods

Description of the Site

In Niger, most of the irrigable land, about 100,000 ha, is located on the alluvial terraces and the low fans of the Niger River. In the river valley, there are many small irrigated zones from 50 to 500 ha. Lossa, the site of this study, is situated 75 km northwest of Niamey, on the left bank of the river (Figure 1). The rainy season, from mid-June to mid-September, provides an annual rainfall (R) of about 400 mm, whereas the annual potential evapotranspiration (ET_0) is in the range of 2100–2200 mm. The result is a highly negative $R - ET_0$.

The region is characterized by the following sequence of geomorphological features: the crusted plateau; the residual sedimentary surfaces of the "continental terminal" series; a sloping (3–5%) fan; a second, less steep (0.3–0.5%) fan; an initial sandy levee; an initial alluvial terrace; a discontinuous sandy levee; and a low flood-prone terrace exclusively used for growing rice. The Lossa site includes the low fan and soils produced by weathering of the metamorphic bedrock of the "Liptako-Gourma."

Soils

The alkali soils (AS) are less suitable for crop production than the brown steppe soils (BSS), alongside which AS are generally found. The boundary between the AS and the BSS is very abrupt (figure 2), as was observed along a 7-m-long and 1.20-m-deep pit dug after a thorough soil survey (Barbiero, 1994b). The study of the contact area using a

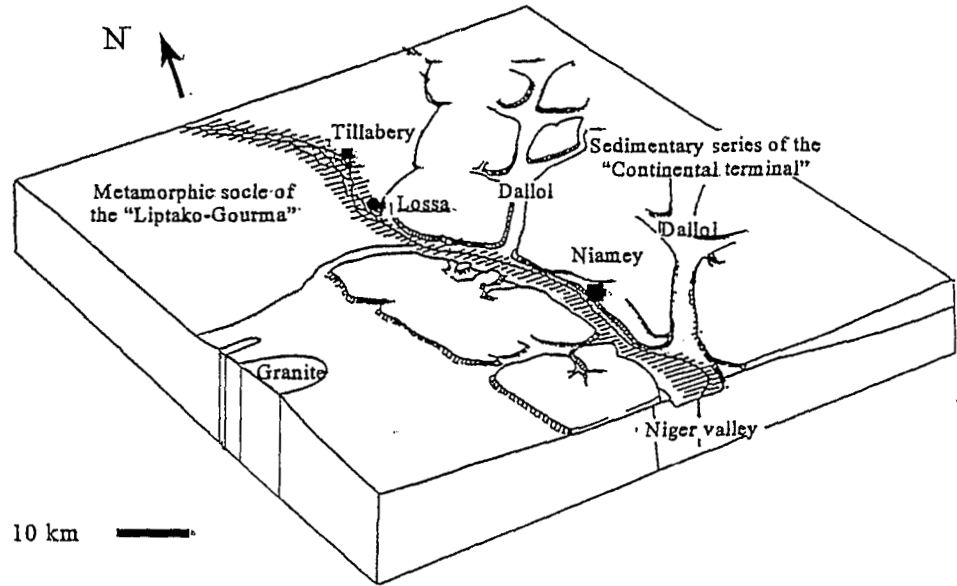


Figure 1. Simplified pattern of the geomorphological features of west Niger in the region of Niamey.

structural approach, was performed to show that it corresponds to a natural transformation of AS into BSS.

Between 20 and 80 cm in depth, the alkali soils are characterized by a grayish material with a sandy-clay-like texture and a coarse, compact structure composed of prisms (50–80 cm wide). The clayey fraction is composed of a mixture of smectites, kaolinites, and to a lesser extent, illites. Smectites, which are the most important, increase along with the depth (Figure 3). This soil type is characterized by a saturated soil paste of pH from 8.4 to 9.8, an exchangeable sodium percentage (ESP) more than 10%, a moderate to weak electrical conductivity from 0.02 to 0.04-S m⁻¹ as saturated paste, and a very low hydraulic conductivity, less than 10⁻⁸ m-s⁻¹. It is sandwiched between a sandy epipedon and a weathered bedrock material rich in calcareous precipitations of different orders (septaria, pseudomycelium veil). The bedrock, made up of a calco-alkaline gneiss to biotite at

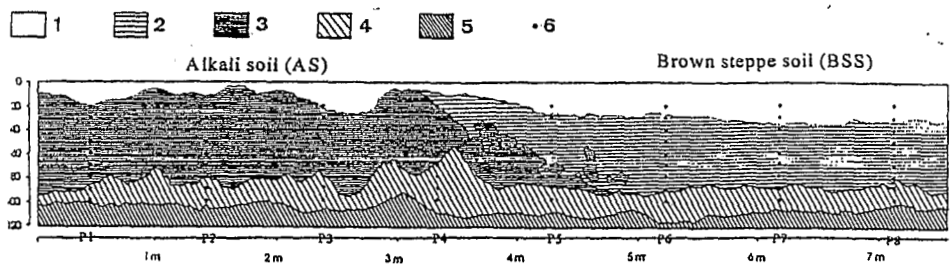


Figure 2. Profile description and transition between alkali and brown steppe soils: 1, sandy epipedon; 2, brown sandy clay loam horizon; 3, gray sandy clay loam horizon; 4, calcareous weathered horizon; 5, weathering horizon with preserved petrographic structure; and 6, chemical analysis sampling points.

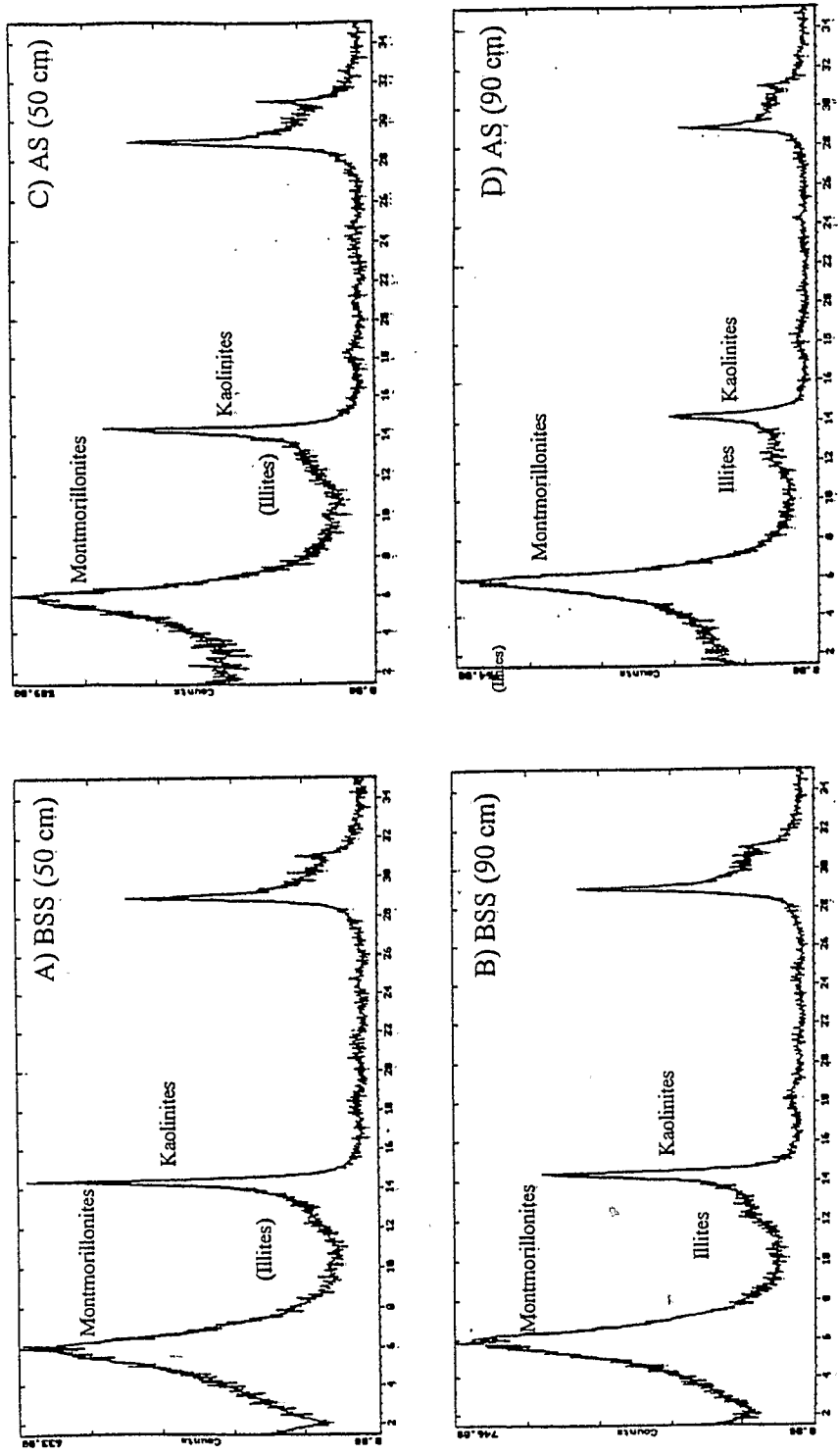


Figure 3. Mineralogical composition of clayey fraction (X-ray diffraction) in alkali (AS) and brow steppe soils (BSS): (a) BSS at 50 cm; (b) BSS at 90 cm; (c) AS at 50 cm; and (d) AS at 90 cm.

around 1-m depth, has a well-preserved petrographic structure and does not present lateral facies variations.

The BSS display a different morphology. The sandy surface layer is thicker, and the underlying horizon of brown soil has a prismatic (10 cm) structure and cubic (1–2 cm) substructure. This material is characterized by a saturated soil paste of pH around 7.0, a low electrical conductivity less than 0.01 S m^{-1} as saturated paste and a hydraulic conductivity of more than 10^{-7} ms^{-1} . The alterite is poorer in calcite crystals, which present many dissolution figures near the transition front. The smectite ratio is less than in alkali soils (Figure 3).

Chemical Analysis

Seventy-two soil samples were obtained along the 7-m-long, 1.2-m-deep pit, at the rate of 8 profiles (P1–P8) that were each 0.95 m lengthwise and 9 samples that were each 0.10 m depthwise from 0.20 m in depth, as indicated in Figure 2. This allows the geochemical variations involved in lateral and vertical transformations to be studied at the same time. This field remained free from irrigation. Saturated soil pastes were prepared; pH was measured after 10 min of agitation when pH and electrical conductivity were stabilized. The soil solution was extracted 24 hours later. The components were analyzed using ion chromatography. A first analysis, with a diluted mixture of Na_2CO_3 and NaHCO_3 at pH 7.0, showed seven peaks for the anions: F^- , Cl^- , NO_2^- , NO_3^- , PO_4^{3-} , SO_4^{2-} and oxalates; and four peaks for the cations: Ca^{2+} , Mg^{2+} , K^+ , and Na^+ . To distinguish F^- from two organic anions (formate and acetate), a second analysis was made with Na-tetraborate as eluant. Another problem concerns numerous complex species, such as CaHCO_3^+ , CaOH^+ , CaCO_3^0 , or CaSO_4^0 for Ca, that cannot be quantified. Thus we used a thermodynamic model AQUA, derived from GYPSOL (Valles & Bourgeat, 1988), to calculate the proportions of these complex species and correct the analysis.

Alkalinity was assessed by assuming electric neutrality of the solution; the validity of this assumption was tested by checking estimates against results obtained by titration. H_4SiO_4^0 was determined by colorimetry using Na-molybdate at pH 1.6 (Charlot, 1961). The major components Ca^{2+} , Mg^{2+} , K^+ , Na^+ , F^- , Cl^- , SO_4^{2-} , H_4SiO_4^0 and the alkalinity were taken into account in further interpretations.

Results and Discussion

Soil Geochemistry of the Low Fan

Soil solution concentration is assessed with a chemical tracer, which is not supposed to interact with its environment. Cl^- is successfully used if it is abundant in the soil solution (Guedarri, 1984; Vallès, 1987; Laraque, 1991), whereas with a weakly concentrated water in Cl^- , other chemical traces are more advisable: K^+ (Guedarri, 1984), ionic strength of solution (N'diaye, 1987), Mg^{2+} (Loyer, 1989), or amount of cations (Gonzalez-Barrios, 1992). The concentration diagram (Figure 4) displays the results of the chemical analysis as functions of increasing sodium ion content, used as tracer. The concentration factor (CF) is then defined as

$$\text{CF} = \frac{[\text{Na}]}{[\text{Na}]_0}$$

where $[\text{Na}]$ is the Na molality and $[\text{Na}]_0$ is the lower Na molality at the origin of the concentration diagram.

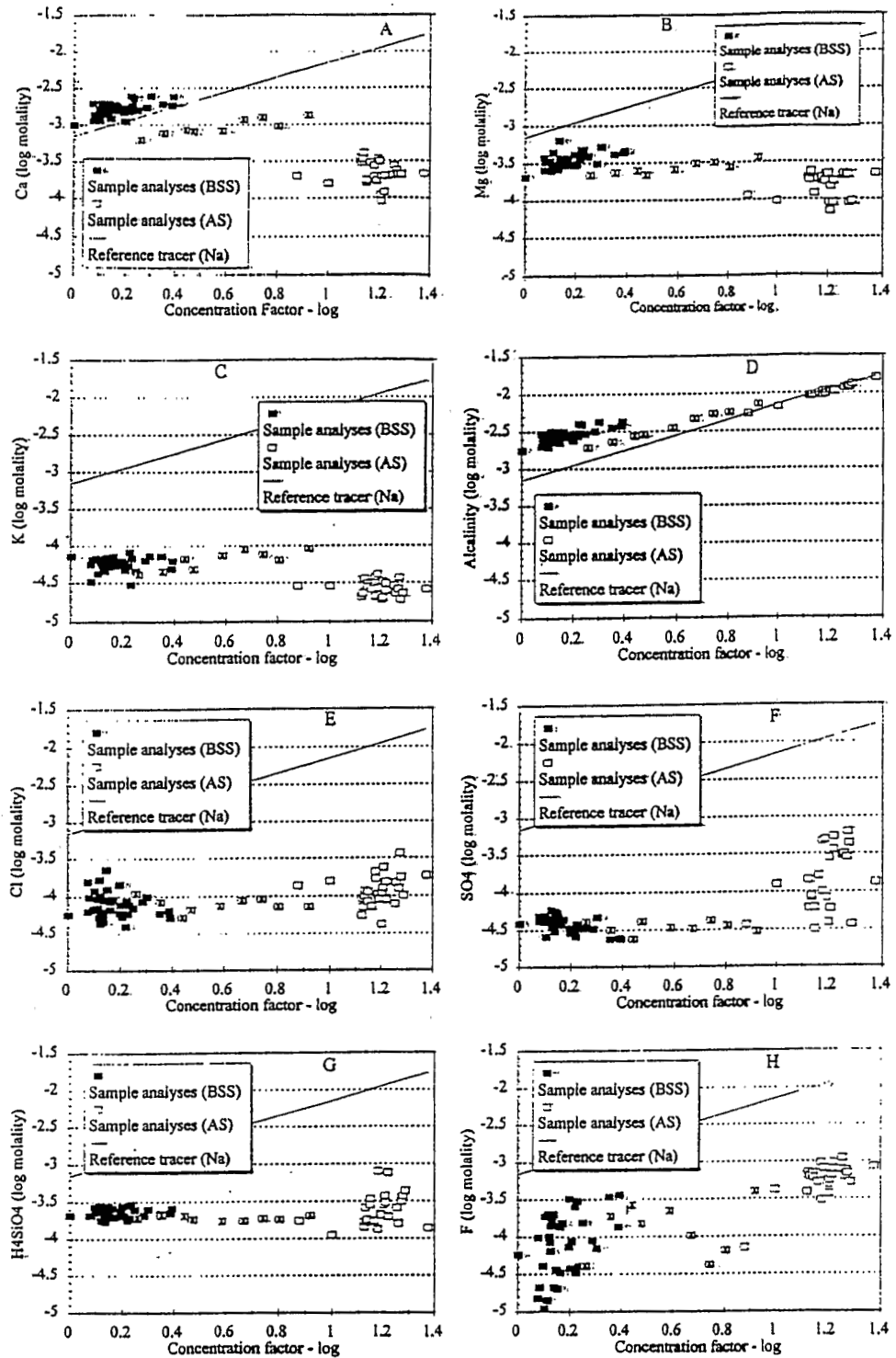


Figure 4. Concentration diagram of the soil solution: (a) Ca^{2+} molality, (b) Mg^{2+} molality, (c) K^{+} molality, (d) alkalinity, (e) Cl^{-} molality, (f) SO_4^{2-} molality, (g) H_4SiO_4^0 molality, and (h) F^{-} molality. Solid squares are sample analyses for BSS; open squares are sample analyses for AS; open squares with cross are profile P4; and diagonal lines are sodium molality as reference tracer for assessed concentration factor.

The AQUA model, derived from GYPSOL (Vallès & Bourgeat, 1988), was used to calculate the activity of dissolved species from their concentrations. The activities provided an indication about the degree of saturation of the sample solutions with the minerals likely to dissolve or precipitate in the soil.

The soil solutions showed distinct geochemical facies, from bicarbonate-calcic type for BSS to bicarbonate-sodic type for AS. F^- were found to be a major component. Typically, F^- is present in lesser amounts in soil solutions, except for alkaline brines from East Africa, where Guedarri (1984) and Chernet and Travi (1993) proved fluorite precipitation. Figure 4 illustrates that concentration of major ions increases less quickly than that of Na^+ ; different types of behavior may be distinguished. Alkalinity and F^- concentration increase consistently, but less rapidly than Na^+ concentration; Ca^{2+} , Mg^{2+} , and K^+ concentrations fall; data points for Cl^- and SO_4^{2-} are disperse, but increasing concentrations can be discerned at high Na^+ concentrations; an initial, approximately constant $H_4SiO_4^0$ molality is followed by an increase at elevated concentration factors.

Soil alkalinity and F^- content appear to be controlled by a geochemical mechanism; they display behavior of the majority ions according to the concept of RA. The saturation diagram in which the analytical results are plotted against calcite (Figure 5a) indicates that this mineral achieves saturation, whereas fluorite (calcium fluoride, CaF_2) achieves saturation for alkali soils only (Figure 5b). In that case the precipitation of fluorite is concomitant with that of calcite. Hence F^- also plays a part in controlling Ca^{2+} molality in the soil solution. In Figure 5a the data points show an oversaturation with respect to calcite. This typical result has been described in several reports (Gac, 1979; Dosso, 1980; Vallès, 1987; Barbiero, 1994a). Ribolzi et al. (1993) showed that it could be attributed to the precipitation of calcite and to thermodynamic disequilibrium, both pointing to the presence of dissolved CO_2 in aqueous solution.

Microanalysis conducted on the calcareous deposits removed from the profiles indicates a Mg^{2+} content of 2% for AS and 2.25% for BSS (Table 1); evaporation studies of water from the Chari River in Chad reveals similar proportions of Mg^{2+} in calcite (Gac, 1979). The Mg^{2+} detected in calcite does not fully account for the strict control of Mg^{2+} molality observed in Na^+ -rich solutions, where a reduction in Mg^{2+} content accompanies an increase in $H_4SiO_4^0$ content. Previous work in Chad (Gac, 1979) and Mali (Vallès et al., 1989) concerned the precipitation of Mg-silicates, and this possibility should also be considered. Our soil solutions were not analyzed for Al^{3+} ; hence the degree of saturation of magnesian aluminum silicates could not be determined precisely. However, Figure 5c indicates that sepiolite achieves saturation; thus it is likely that closely related magnesian aluminum silicates (montmorillonite-Mg) do precipitate. Simple thermodynamic models are inadequate to explain the diminution of K^+ molality. Its adsorption cannot explain the geochemical control exerted on K^+ because the exchangeable potassium percentage falls when the soil solution is concentrated. Illite precipitation could explain the K^+ control. Thus we assessed Al^{3+} activity in the soil solution, supposedly in equilibrium with kaolinite. Figure 5d indicates that illite does not achieve saturation. However, the undersaturation is low, and the trend of the data parallels that of the theoretical equilibrium line. It proves that a closely related K-silicate with a similar composition and a lower solubility does precipitate.

$H_4SiO_4^0$ molality remains surprisingly undersaturated with respect to amorphous silica, abundant in these soils. Slow dissolving of amorphous silica (Iler, 1979; Dandurand et al., 1982) could explain this phenomenon and the apparent disequilibrium of the extracts from saturated soil pastes with respect to amorphous silica. $H_4SiO_4^0$ should be issued from the partial dissolution of clayey minerals that could lead to progressively equilibrate the soil paste with respect to the existing silicates.

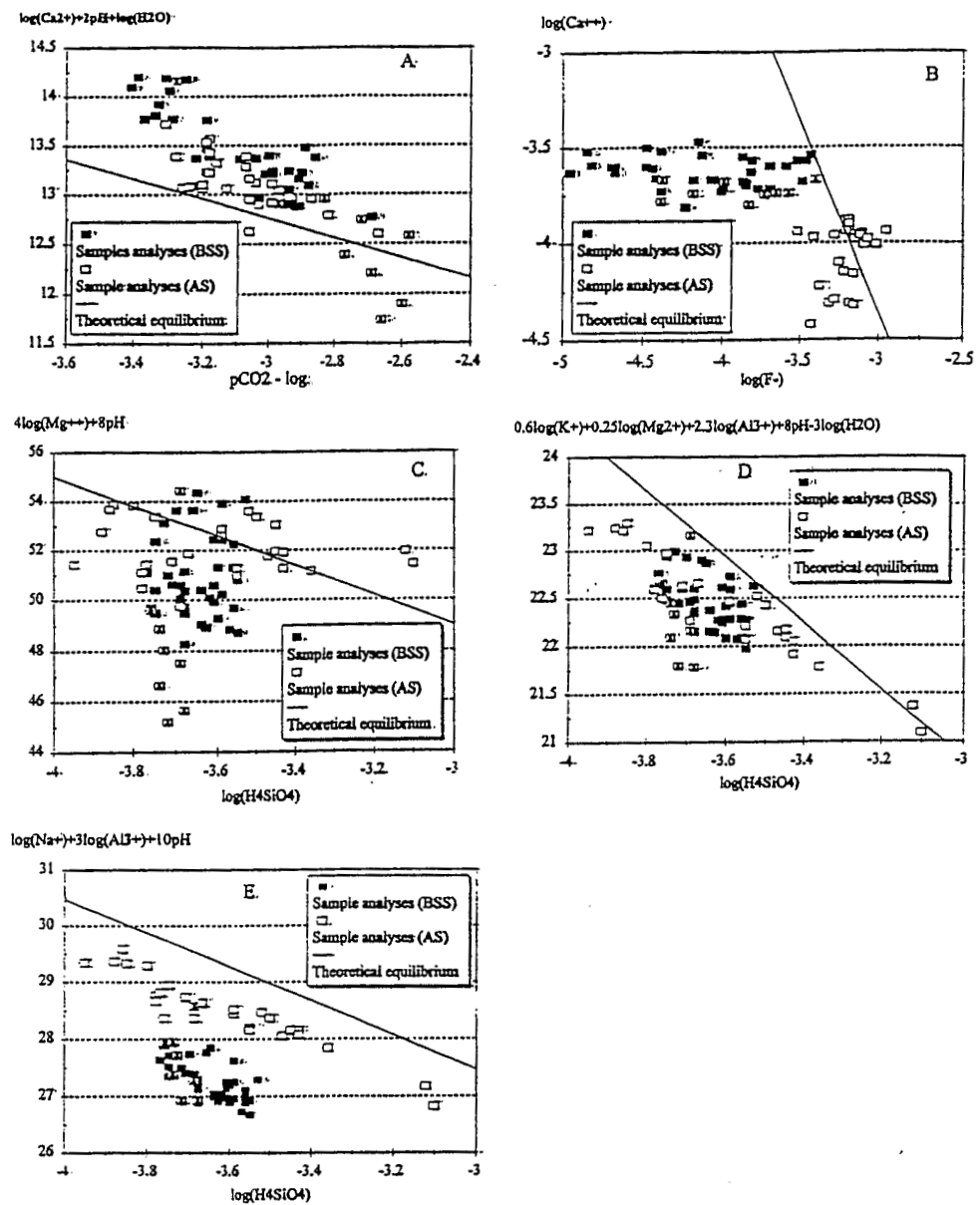


Figure 5. Equilibrium diagram of soil solutions with respect to (a) calcite, (b) fluorite, (c) sepiolite, (d) illite, and (e) paragonite. Solid squares are sample analyses for brpwn steppe soils (BSS); open squares are sample analyses for alkali soils (AS); open squares cross are profile P4; and diagonal lines are theoretical equilibrium.

The trend in Cl^- and SO_4^{2-} does not parallel that of Na^+ . None of the species achieved a significant degree of saturation on-site; this behavior cannot be accounted for by geochemical control. The statistical and geostatistical study of the vertical distribution (Barbiero, 1994a) showed a concentration gradient toward the upper reach of the profiles for both Cl^- and SO_4^{2-} , whereas the other species and the total dissolved charge show a concentration gradient toward the bottom, the maximum occurring at the alteration band

of the bedrock. The higher Cl^- and SO_4^{2-} contents are therefore due to a contribution from the top of the profile, probably from runoff. Since Cl^- and SO_4^{2-} differ in origin from the other species, this could explain the wider dispersion of data points on the concentration diagram, and the concentration trend, which appears to be unrelated to that of Na^+ . The low concentration of the runoff water and the mechanisms of control of cations in the soil explain the narrow dispersion of the cations accompanying Cl^- and SO_4^{2-} in the runoff water. On the other hand, the study of lateral distribution proved that the transformation of AS into BSS concerns geochemical features rather than morphological features (Barbiero, 1994b), as illustrated by the case of profile P4 in Figures 2, 4, and 5.

Simulation

Our explanations might not be quite adequate because of the low solubility of the amorphous silica and the fast variations of $p\text{CO}_2$ in solution, which induce obvious problems of representation. With the exception of amorphous silica, the equilibrium conditions of these different minerals are strongly affected by the pH and the partial pressure of dissolved CO_2 in the soil solution. While $p\text{CO}_2$ decreases in the saturated paste or the extract, pH increases, and the solution appears oversaturated with respect to the identified minerals. At the same time, the slow dissolving of amorphous silica induces an undersaturation with respect to silicates. This disequilibrium is balanced by calcite precipitation and silicate dissolution in the 24-hour saturated soil pastes. Thus we assessed $p\text{CO}_2$ to achieve the equilibrium of the soil solution with respect to calcite, sepiolite, illite, kaolinite, and amorphous silica. The $p\text{CO}_2$ was found close to $10^{-2.6}$.

The AQUA model was used to simulate Ca^{2+} , Mg^{2+} , K^+ , and Na^+ molalities and alkalinity along the concentration process. At each step, equilibrium is calculated by minimization of Gibbs free energy. Calcite, sepiolite, and illite precipitation was allowed. Soil solution is assumed to be in equilibrium with respect to amorphous silica and kaolinite. The dissolution reactions and thermodynamic constants are listed in Table 2.

A part of the concentration diagram, simulated with the successive precipitations of calcite, illite, and sepiolite, agrees with the analytical results. However, above a concentration factor of 16, the simulated concentration of Na^+ quickly exceeds the measured concentrations. This assumes a mechanism of Na^+ control. The Ca^{2+} , Mg^{2+} , and Na^+ exchanges with the adsorbing complex have been taken into account in the further simulations. Constant selectivity coefficients were considered: 11 and 1 for sodium-calcium

Table 1
 Ca^{2+} and Mg^{2+} proportions in calcite for alkali (AS) and brown steppe soils (BSS)

Soil type	Sample	$\text{Ca}^{2+}(\%)$	$\text{Mg}^{2+}(\%)$
AS	1	96.6	1.9
	2	96.4	2.2
	3	95.7	1.9
	Mean	96.2	2.0
BSS	1	95.8	2.3
	2	96.4	2.2
	Mean	96.1	2.25

Table 2
Dissolution reaction of minerals—thermodynamic data

Mineral	Dissolution reaction	pK
Calcite	$\text{CaCO}_3 \rightleftharpoons \text{Ca}^{2+} + \text{CO}_3^{2-}$	-8.73 ^a
Amorphous silica	$\text{H}_4\text{SiO}_4 \rightleftharpoons \text{H}_4\text{SiO}_4^0$	-2.71 ^b
Sepiolite	$\text{Si}_6\text{Mg}_4\text{O}_{15}(\text{OH})_2 \cdot 4\text{H}_2\text{O} + 8\text{H}^+ + 3\text{H}_2\text{O} \rightleftharpoons 4\text{Mg}^{++} + 6\text{H}_4\text{SiO}_4^0$	+31.0 ^c
Illite	$\text{Si}_{35}\text{Al}_{23}\text{Mg}_{0.25}\text{O}_{10}(\text{OH})_2\text{K}_{0.6} + 8\text{H}^+ + 3\text{H}_2\text{O} \rightleftharpoons 0.6\text{K}^+ + 2.3\text{Al}^{3+} + 0.25\text{Mg}^{2+} + 3.5\text{H}_4\text{SiO}_4^0$	+10.34 ^b
Kaolinite	$\text{Si}_2\text{Al}_2\text{O}_5(\text{OH})_4 + 6\text{H}^+ \rightleftharpoons 2\text{Al}^{3+} + 2\text{H}_4\text{SiO}_4^0 + \text{H}_2\text{O}$	+7.43 ^b
Fluorite	$\text{CaF}_2 \rightleftharpoons \text{Ca}^{2+} + 2\text{F}^-$	-10.37 ^d
Paragonite	$\text{Si}_3\text{Al}_5\text{O}_{10}(\text{OH})_2\text{Na} + 10\text{H}^+ \rightleftharpoons \text{Na}^+ + 3\text{Al}^{3+} + 3\text{H}_4\text{SiO}_4^0$	+18.47 ^b

^aHelgeson (1969).

^bFritz (1981).

^cHelgeson et al. (1978).

^dBarbiero (1994a).

and calcium-magnesium exchanges, respectively, in the Gaines and Thomas (1953) convention; a CEC of 0.123 mol kg⁻¹ of soil; a porosity of 40%; and a bulk density of 1.6. If the ionic exchanges explain a temporary control of Na⁺ molality increase, then we have to consider the precipitation of an Na-silicate to explain that the sodium has reached its top. The saturation diagram (Figure 5e), in which the analytical results are plotted, indicates that the soil solution remains undersaturated with respect to paragonite (Table 2). Nevertheless, the trend of the most concentrated analysis parallels that of the theoretical equilibrium line and shows that geochemical control of Na⁺ exists. Thus we supposed that the soil solution is in equilibrium with kaolinite and amorphous silica and that $p\text{CO}_2 = 10^{-2.6}$, as estimated previously. We assessed a pK of 17.21 to achieve saturation, instead of 18.47 for the paragonite dissolution.

As the initial solution is concentrated 100 times, Ca²⁺, Mg²⁺, K⁺, and Na⁺ molalities and alkalinity are controlled by the precipitation of calcite and Mg, K, and Na silicates. Thus, when the concentration continues, the soil solution does not vary, while the amount of these minerals increases at the expense of the kaolinite. This result is consistent with the mineralogical properties of the AS and BSS (Figure 3). The Na⁺ molality was used as a concentration factor. This simulated concentration diagram agrees with the analytical results (Figure 6) except for

- an overestimation of alkalinity (Figure 6d) in the low concentration range due to the lack of others anion species in the simulation;
- an underestimation of K⁺ (Figure 6c) and Mg²⁺ (Figure 6b) molalities in the high concentration range due to an undersaturation and a feasible dissolution of silicates in the saturated soil pastes; and
- an overestimation of Ca²⁺ (Figure 6a) molalities in the high concentration range due to an oversaturation and a feasible precipitation of calcite in the saturated soil pastes and the extracts.

Representativity of Lossa's Soils to Other Regional Soils

When the soil solution becomes more concentrated, Ca²⁺ and, to a lesser extent, Mg²⁺ molalities fall, whereas Na⁺ molality increases. The base exchange complex of the soil

then equilibrates with the solution through Na^+ adsorption: Gavaud (1977) pointed out that, in this region, the local saturation percentage of Na^+ can reach 40%, which is consistent with the analytical results obtained during the initial survey. As our soil solutions, and those of the survey, displayed the same chemical characteristics and covered the same concentration ranges, the geochemical mechanisms postulated for the Lossa sampling site can be extended to the wider area covered by the survey. Two factors appear to influence the geochemistry of the soils from the low fan (Lossa): alteration of the parent rock from calco-alkaline gneiss to biotite, and to a lesser extent, local runoff. A mechanism for the formation of these soils has been proposed by Barbiero (1994b); it can explain the highly localized alkalinization in plots of several hectares.

Analytical results from the alluvial terraces at Sona were also studied (Feau, 1976). They are close to our results for the Lossa site and cover the same concentration range. However, the chemical characteristics are acquired differently. At Sona the geochemistry is not directly attributable to alteration of the base: alluvial deposits are frequently found resting on unaltered rock at several meters depth. The elongated alkali soil units are generally located upriver from the levee of the Niger. It is possible that the chemical similarity of the soils, on the fans and on the alluvial deposits, is the result of water flowing from the deposits on the base toward the alluvial terrace. The possibility that a former river table existed at a much lower depth than that of the present river can also be considered. As the chemical facies of the water table was similar to that of the soil solution, but less concentrated, capillary rise from the water table would have resulted in

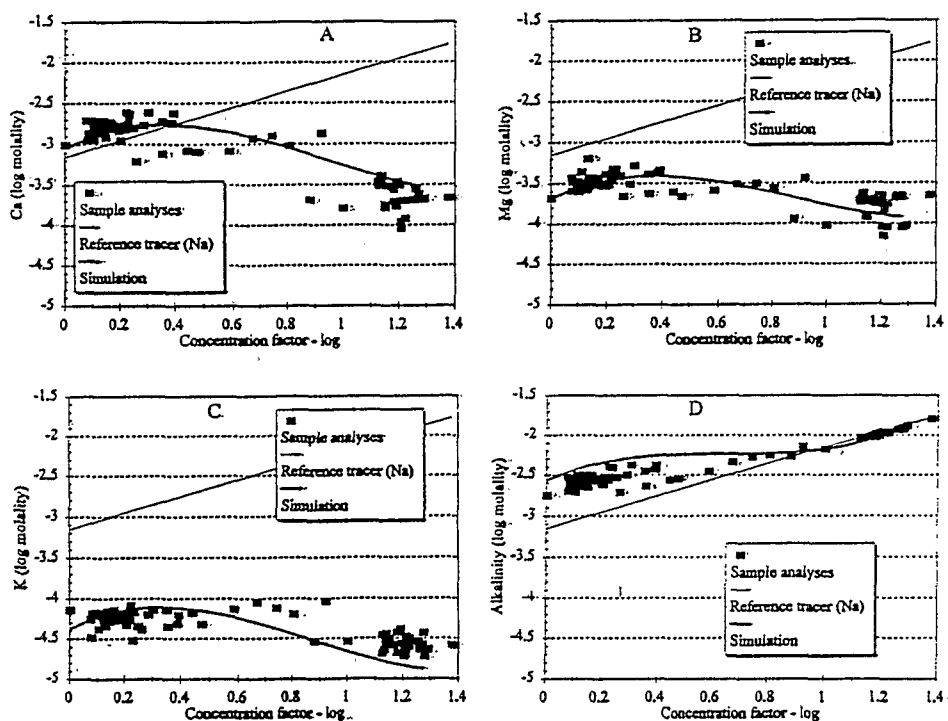


Figure 6. Simulation of the concentration of the soil solution with Na^+ molality as estimated concentration factor: (a) Ca^{2+} molality, (b) Mg^{2+} molality, (c) K^+ molality, and (d) alkalinity. Solid squares are sample analyses; diagonal lines are sodium molality as reference tracer for estimated concentration factor; and curves are the simulation.

the formation of the appropriate soil units. However, this hypothesis cannot explain the very abrupt transitions between the alkali soils and other soil units on the alluvial terrace. A detailed study of the distribution of alkaline character at this site is required to identify the soil genesis.

To check whether these geochemical mechanisms were representative of the region, we compared our results with those obtained at Namarde Goungou, which is located about 20 km downriver on the low flood-prone terraces (Guero, 1987). Although the soil solution from Namarde Goungou was more concentrated, the soils were found to belong to the same chemical family as those from Lossa and Sona.

Conclusion

On the low fan, alkalization and sodization are related to the concentration of the alteration products and to insufficient lixiviation of salts. The precipitation of calcite to produce positive residual alkalinity starts the geochemical process. It results in low concentration of Ca^{2+} and in alkalization: Ca^{2+} desorption is accompanied by adsorption of Na^+ on the exchange complex. The low fan provided original evidence for the precipitation of fluorite, which also contributes to geochemical control of Ca^{2+} in solution. Mg^{2+} , K^+ , and Na^+ molalities in the soil solution are controlled by the formation of silicates and by exchanges. These silicates belong to the illite and smectite types, but further investigations are necessary to specify their mineralogical features. These results were validated by simulation of the concentration process. The increasing alkaline reserve corresponds with

- an increase of the alkalinity in soil solution, which affects the chemical properties and the pH;
- on the exchange complex, a storage of Na^+ associated with a loss a Ca^{2+} , liable to neutralize alkalinity. This sodization slows down the evolution of the soil solution because the cations fixed on the exchange complex are, at least, 40 times more abundant than those in the soil solution; it entails a degradation of the physical properties;
- a storage of silicates under alkaline conditions, which store cations and hydroxyl ions, and thus alkalinity. These mineralogical modifications might correspond to a very important stock of alkalinity which prevents the rehabilitation of these alkali soils.

Soil solutions from the fan and from the first alluvial terraces display similar chemical characteristics. Since the waters belong to the same chemical family, it is possible that identical geochemical mechanisms are involved in the formation of alkali soils at the three sites of Lossa, Sona, and Namarde Goungou.

References

- Barbiero, L. 1994a. Les sols alcalinisés sur socle dans la vallée du fleuve Niger: origine de l'alcalinisation et évolution des sols sous irrigation. Doctoral thesis, ENSA, Rennes, France.
- Barbiero, L. 1994b. Mise en évidence d'une désalcalinisation naturelle des sols en région tropicale. Transformation de sols alcalins en sols bruns subarides dans un bas-fond sahélien du Niger. *Comptes Rendu d'Académie Sciences Paris*. 319, série II:659-665.
- Bourrié, G. 1976. Relations entre le pH, l'alcalinité, le pouvoir tampon et les équilibres de CO_2 dans les eaux naturelles. *Science du Sol* 3:141-159.

- Charlot, G. 1961. *Dosages colorimétriques des éléments minéraux. Principes et méthodes*. Masson, Paris.
- Chernet, T., and Y. Travi. 1993. Preliminary observations concerning the genesis of high fluoride contents in the Ethiopian Rift, pp. 651–655, in U. Thorweihe and H. Schandelmeier, eds., *Geoscientific research in northeast Africa*. Balkema, Rotterdam.
- Dandurand, J. L., J. Mizele, J. Schott, F. Bourgeat, V. Vallès, and Y. Tardy. 1982. Premiers résultats sur la solubilité de la silice amorphe dans les pores de petite taille. Variation du coefficient d'activité de la silice en fonction de l'activité de l'eau. *Sciences Géologiques Mémoire 35*, pp. 11–79. Université Louis Pasteur, Strasbourg.
- Dosso, M. 1980. Géochimie des sols salés et des eaux d'irrigation. Aménagement de la basse vallée de l'Euphrate en Syrie. Doctoral thesis, INP Toulouse.
- Droubi, A. 1976. Géochimie des sels et des solutions concentrées par évaporation. Modèle thermodynamique de simulation. Application aux sols salés du Tchad. *Sciences Géologiques Mémoire 46*, p. 177, Université Louis Pasteur, Strasbourg.
- Eaton, F. M. 1950. Significance of carbonates in irrigation waters. *Soil Science* 69:123–133.
- Feau, C. 1976. Etude pédologique des périmètres de Lossa et Sona. Rapport INRAN/GERDAT. Niamey, Niger.
- Fritz, B. 1981. Etude thermodynamique et modélisation des réactions hydrothermales et diagénétiques. *Sciences Géologique Mémoire 65*, Université Louis Pasteur, Strasbourg.
- Gac, J. Y. 1979. Géochimie du bassin du lac Tchad. Bilan de l'altération, de l'érosion et de la sédimentation. Doctorat thèse, 249 pp., Université Louis Pasteur, Strasbourg.
- Gac, J. Y., A. Droubi, B. Fritz, and Y. Tardy. 1977. Geochemical behaviour of silica and magnesium during the evaporation of waters in Chad. *Chemical Geology* 19:215–228.
- Gaines, G. L., and H. C. Thomas. 1953. Adsorption studies on clay minerals: II. A formulation of the thermodynamics of exchange adsorption. *Journal of Chemical Physics* 23:2322–2326.
- Gavaud, M. 1977. Les grands traits de la pédogénèse au Niger méridional. *Travaux Documentaires 76*, ORSTOM, Paris.
- Gonzalez-Barrios, J. L. 1992. Eau d'irrigation et salinité des sols en zone aride mexicaine. Exemple de la "Comarca Lagunera." Doctorat thèse, USTL Montpellier.
- Guedarri, M. 1984. Géochimie et thermodynamique des évaporites continentales. Etude du lac Natron en Tanzanie et du Chott el Jerid en Tunisie. *Sciences Géologiques Mémoire 76*, Université Louis Pasteur, Strasbourg.
- Guero, Y. 1987. Organisation et propriétés fonctionnelles des sols de la vallée du moyen Niger. Doctorat thèse, Université de Niamey et Tunis.
- Helgeson, H. C. 1969. Thermodynamics of hydrothermal systems at elevated temperatures and pressure. *American Journal of Science* 267:724–804.
- Helgeson, H. C., J. M. Delany, H. W. Nesbitt, and D. K. Bird. 1978. Summary and critique of the thermodynamic properties of rock-forming minerals. *American Journal of Science* 278-A–229.
- Iler, R. K. 1979. *The solubility of silica*. John Wiley, New York.
- Laraque, A. 1991. Comportements hydrochimiques des açudes du nordeste brésilien semi-aride. Evolution et prévision pour un usage en irrigation. Doctorat thèse, USTL, Montpellier.
- Loyer, J. Y. 1989. Les sols salés de la basse vallée du fleuve Sénégal. Caractérisation, distribution et évolution sous culture. Collection étude et thèses, ORSTOM, Paris.
- N'diaye, M. K. 1987. Evaluation de la fertilité des sols à l'office du Niger (Mali). Contribution à la recherche des causes et origines de la dégradation des sols dans le kouroumari. Doctorat thèse, INP Toulouse.
- Ribolzi, O., V. Vallès, and L. Barbiero. 1993. Contrôle géochimique des eaux par la formation de calcite en milieu méditerranéen et en milieu tropical. Arguments d'équilibre et arguments de bilan. *Science du Sol* 31(1/2):77–95.
- Tardy, Y. 1985. *Le cycle de l'eau*. Masson, Paris.
- Vallès, V. 1987. Etude et modélisation des transferts d'eau et de sel dans un sol argileux. Appli-

- cation au calcul des doses d'irrigation. *Sciences Géologiques Mémoire 79*. Université Louis Pasteur, Strasbourg.
- Vallès, V., and F. Bourgeat. 1988. Geochemical determination of the gypsum requirement of cultivated sodic soils, I. Development of the thermodynamic model GYPSOL simulating the irrigation water-soil chemical interaction. *Arid Soil Research and Rehabilitation* 2:165-177.
- Vallès, V., M. K. N'diaye, A. Bernadac, and Y. Tardy, 1989. Geochemistry of water in the Kouroumari region, Mali. Al, Si and Mg in waters concentrated by evaporation: Development of a model. *Arid Soil Research and Rehabilitation*, 3:21-39.
- Vallès, V., Y. A. Pachepsky, and A. A. Ponizovsky. 1991. Invariant criteria for irrigation water quality assessment in arid and semi-arid regions. Genesis and control of fertility of salt affected soils, pp. 330-333, in V. V. Dokuchaev, ed., *ISSS Subcommission on Salt Affected Soils Science*. Soil Institute, Moscow.
- van Beek, C. G. E., and N. van Breemen. 1973. The alkalinity of alkali soils. *Journal of Soil Science* 24:129-136.